

Supplementary Materials: Electronic Communication between Dithiolato-Bridged Diiron Carbonyl and S-Bridged Redox-Active Centres

Cédric Tard ¹, Stacey J. Borg ², Shirley A. Fairhurst ³, Christopher J. Pickett ^{4,*} and Stephen P. Best ^{5,*}

¹ LCM, CNRS, Ecole Polytechnique, Université Paris-Saclay, 91128 Palaiseau Cedex, France; cedric.tard@polytechnique.edu

² School of Chemistry, The University of Melbourne, Parkville, Victoria 3010, Australia; staceyborg@gmail.com

³ School of Chemistry, University of East Anglia, Norwich NR4 7TJ; s.fairhurst@uea.ac.uk

⁴ School of Chemistry, University of East Anglia, Norwich NR4 7TJ; c.pickett@uea.ac.uk

⁵ School of Chemistry, The University of Melbourne, Parkville, Victoria 3010, Australia; spbest@unimelb.edu.au

* Correspondence: spbest@unimelb.edu.au; (S.P.B.), c.pickett@uea.ac.uk; (C.J.P.)

Received: date; Accepted: date; Published: date

Figure S1 Cyclic voltammogram of (— —) nitrobenzene (2 mM) and (—) CH₃C(CH₂S)₂CH₂S(C₆H₄-p-NO₂) (12) (2 mM) (0.2 M [NBu₄][BF₄] in acetonitrile, 0.1 V.s⁻¹). 2

Figure S2. Cyclic voltammograms of the primary reduction processes of nitrobenzene (2 mM, 0.2 M [NBu₄][BF₄] in acetonitrile, 0.1 V.s⁻¹) in the absence and in the presence of acetic acid: 0 (—), 1 (— —), 5 (---), 15 (----) and 30 equivalents (— - - -). 2

Figure S3. Cyclic voltammogram of 2,6-lutidinium tetrafluoroborate (0.4 M, 0.2 M [NBu₄][BF₄] in acetonitrile, 0.1 V.s⁻¹). 2

Figure S4. IR-SEC single beam spectra recorded during (top) reduction and (bottom) re-oxidation of **I-bzNO₂** in CH₂Cl₂ (2 mM, 0.2 M TBAPF₆). For this, and subsequent, figures the initial spectrum of each block is shown in green and the final spectrum in blue. 3

Figure S5. IR-SEC spectra recorded during (a) the reduction and (b) re-oxidation of **I-bzNO₂** in the presence of HLut⁺. 3

Table S1. EasySpin EPR simulation parameters for [**I-bzNO₂**]⁻.

Table S2. Determination of the free energy activation (ΔG[‡]) parameter in CDCl₃; T_c is the coalescence temperature; Δv_{ab} is determined from the slow limit spectra.

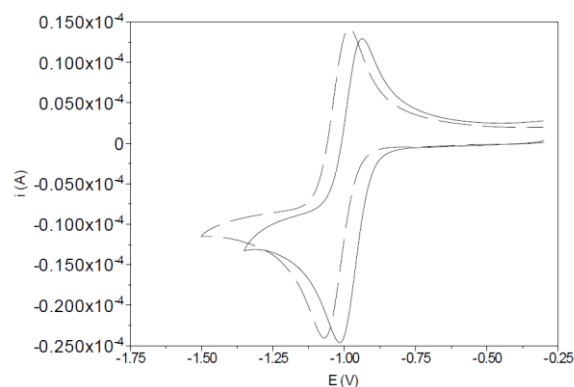


Figure S1 Cyclic voltammogram of (— —) nitrobenzene (2 mM) and (—) $\text{CH}_3\text{C}(\text{CH}_2\text{S})_2\text{CH}_2\text{S}(\text{C}_6\text{H}_4\text{-p-NO}_2)$ (12) (2 mM) (0.2 M $[\text{NBu}_4][\text{BF}_4]$ in acetonitrile, $0.1 \text{ V}\cdot\text{s}^{-1}$).

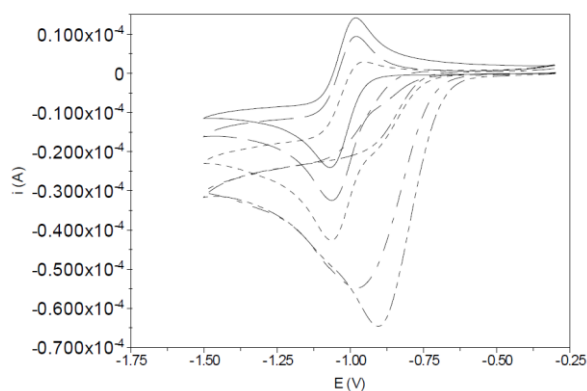


Figure S2. Cyclic voltammograms of the primary reduction processes of nitrobenzene (2 mM, 0.2 M $[\text{NBu}_4][\text{BF}_4]$ in acetonitrile, $0.1 \text{ V}\cdot\text{s}^{-1}$) in the absence and in the presence of acetic acid: 0 (—), 1 (— —), 5 (---), 15 (— · —) and 30 equivalents (— · · —).

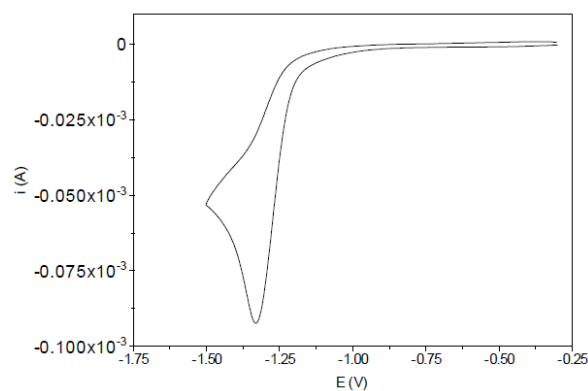


Figure S3. Cyclic voltammogram of 2,6-lutidinium tetrafluoroborate (0.4 M, 0.2 M $[\text{NBu}_4][\text{BF}_4]$ in acetonitrile, $0.1 \text{ V}\cdot\text{s}^{-1}$).

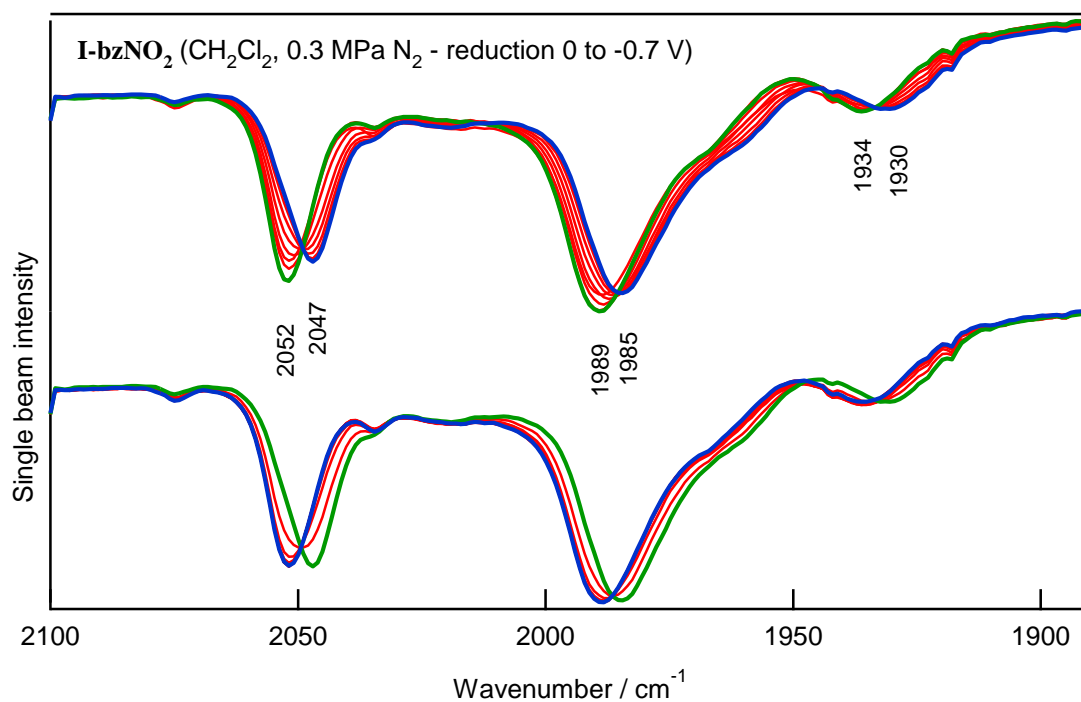


Figure S4. IR-SEC single beam spectra recorded during (top) reduction and (bottom) re-oxidation of **I-bzNO₂** in CH_2Cl_2 (2 mM, 0.2 M TBAPF₆). For this, and subsequent, figures the initial spectrum of each block is shown in green and the final spectrum in blue.

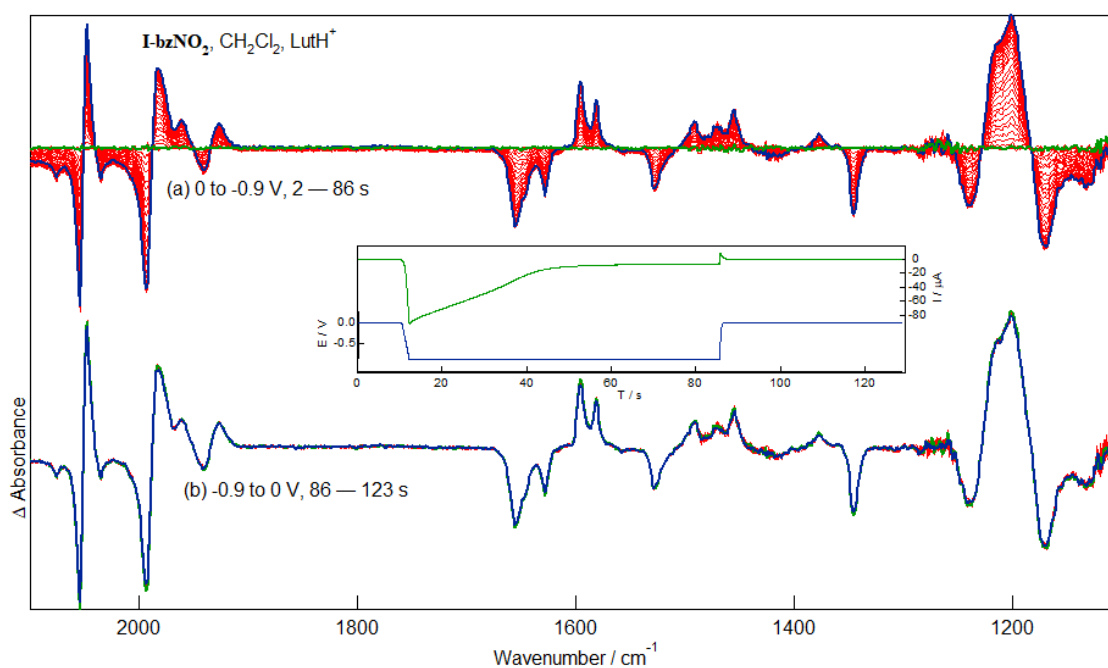


Figure S5. IR-SEC spectra recorded during (a) the reduction and (b) re-oxidation of **I-bzNO₂** in the presence of HLut^+ .

Table S1. EasySpin EPR simulation parameters for [I-bzNO₂]^{•−}.

```

[Bexp,Espc,Params] = eprload('sb_fe2s3no2_hires_1');
Bexp = Bexp/10;
Be = Bexp .';
Bt = Be(3688:6145);
Esp = Espc .';
Espt = Esp(3688:6145);
g = (71.44775 * Params.MF) ./ Be;
Exp.mwFreq = Params.MF;
Exp.Range = [min(Bt) max(Bt)];
Exp.nPoints = size(Bt,1);
Sys.g = 2.00543;
Sys.Nucs = 'N, H, H, H, H, H';
Sys.n = [1 1 1 1 1 2];
Sys.lwpp = [0.08 0.036]*0.65;
An = 24.43;
Ah1 = 10.3;
Ah1p = 8.4;
Ah2 = 3.6;
Ah2p = 2.4;
Sys.A = [An, Ah1, Ah1p, Ah2, Ah2p, 1.4];
[Bsim,Sspc] = garlic(Sys,Exp);
Sspc = 1.5 * Sspc;
subplot(1,1,1), plot(Bt,Espt, Bsim,Sspc);

```

Table S2. Determination of the free energy activation (ΔG^\ddagger) parameter in CDCl₃; T_c is the coalescence temperature; Δv_{ab} is determined from the slow limit spectra.

Compound	Δv_{ab} (Hz)	T_c (K)	ΔG^\ddagger (at T_c) (kJ.mol ^{−1})	ΔG^\ddagger (at T_c) <i>simulated</i> (kJ.mol ^{−1})	ΔH^\ddagger (kJ.mol ^{−1})	E_a (kJ.mol ^{−1})
I-bzNO ₂	20-330*	200	/	38-42	/	/
I-bzNH ₂	323	243	45.8 ± 0.5	45.80	51.7	55.4
I-bzNH ₃ ⁺	315	208	39.0 ± 0.5	38.98	14.2	16.2

* Due to the machine limitation it was not possible to record the slow limit spectra, however coalescence at approximately 200 K was observed and a range of value for ΔG^\ddagger was obtained by simulating the slow limit spectra using the programme gNMR.

NMR experiments were performed in *d*-chloroform and from the data activation energies ΔG^\ddagger for the AB↔A2 spin system of different {2Fe3S}-complexes were calculated at T_c and these are given in Table S1. Simulations of the NMR spectra were also performed and ΔG^\ddagger values (at T_c) are in very good agreement with the experimental data. Simulation of the spectra over a range of temperatures provides further data. ΔH^\ddagger are obtained from the Eyring plot (ln k/T vs. $1/T$) and values of E_a are obtained from an Arrhenius plot (ln k vs. $1/T$), noting that $\Delta H^\ddagger \approx E_a - RT$. In both cases, k values were estimated by simulation of the experimental spectra.